Inorganic Chemistry

Article

pubs.acs.org/IC

Structural and Thermodynamic Study of the Complexes of Nd(III) with *N,N,N′,N′*-Tetramethyl-3-oxa-glutaramide and the Acid Analogues

Guoxin Tian,[†] Simon J. Teat,*[,‡] and Linfeng Rao*[,†]

[†]Chemical Sciences Division, Lawrence Berkeley National Laboratory, Berkeley, California 94720, United States

[‡]Advanced Light Source, Lawrence Berkeley National Laboratory, Berkeley, California 94720, United States

Supporting Information

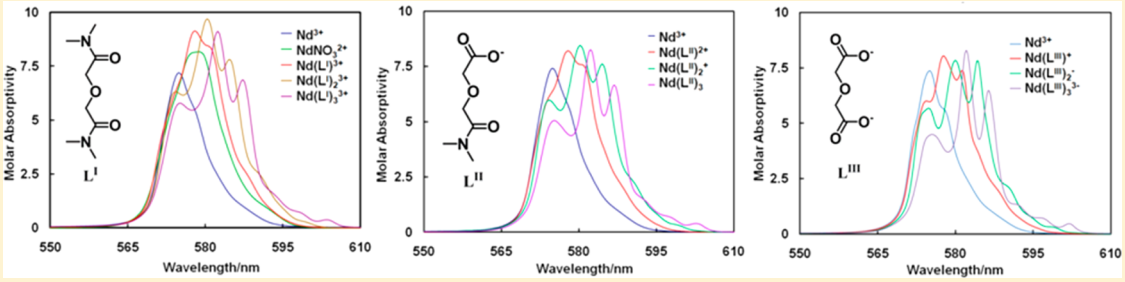

ABSTRACT: The thermodynamics of Nd(III) complexes with *N,N,N′,N′*-tetramethyl-3-oxa-glutaramide (TMOGA, L^I), *N,N*-dimethyl-3-oxa-glutaramic acid (DMOGA, HL^{II}), and oxydiacetic acid (ODA, H_2L^{III}) in aqueous solutions was studied. Stability constants, enthalpies, and entropies of complexation were determined by spectrophotometry, potentiometry, and calorimetry. The stability constants of corresponding Nd(III) complexes decrease in the following order: Nd(III)/L^{III} > Nd(III)/L^{II} > Nd(III)/L^I. For all complexes, the enthalpies of complexation are negative and the entropies of complexation are positive, indicating that the complexation is driven by both enthalpy and entropy. Furthermore, from L^{III} to L^{II}, and to L^I, the enthalpy of complexation becomes more exothermic and the entropy of complexation less positive, suggesting that the substitution of a carboxylate group with an amide group on the ligands enhances the enthalpy-driven force but weakens the entropy-driven force of the complexation with Nd(III). Crystal structures of three 1:3 Nd(III) complexes, $Nd(L^I)_3(ClO_4)_3$ (**I**), $Nd(L^I)_3(NO_3)_3(H_2O)_2$ (**II**), and $Nd(L^{II})_3(H_2O)_{7.5}$ (**III**), were determined by single-crystal X-ray diffraction and compared with the structure of a 1:3 Nd(III)/L^{III} complex in the literature, $Na_3NdL^{III}_3(NaClO_4)_2(H_2O)_6$ (**IV**). In all four structures, the ligands are tridentate and Nd(III) is nine-coordinated with similar distorted tricapped trigonal prism geometry by three ether oxygen atoms capped on the three faces of the prism, and six oxygen atoms from the ketone group or carboxyl group at the corners. The absorption spectra of Nd(III) in solutions showed very similar patterns as Nd(III) formed successive 1:1, 1:2, and 1:3 complexes with L^I, L^{II}, and L^{III}, respectively, implying that the Nd(III) complexes with the three ligands have similar coordination geometries in aqueous solutions, as observed in the solids.

1. INTRODUCTION

Spent nuclear fuel reprocessing helps to minimize the volume and reduce the long-term radioactive toxicity of high-level nuclear wastes from weapons programs and civilian nuclear power plants, to effectively manage global nuclear resources, and to reduce the risk of proliferation of nuclear weapons. The well-known PUREX process has been very successfully used in the separation of uranium and plutonium from the irradiated nuclear fuel in weapons programs, because of the high selectivity of tributyl phosphate (TBP) for U(VI) and Pu(IV) versus minor actinide ions [mainly Np(V), Am(III), and Cm(III)], most fission products, and other components from corrosion and the reagents added during the processes. However, the main advantage of the PUREX process that originates from the good selectivity of TBP for U(VI) and Pu(IV) in weapons programs becomes an obvious disadvantage for civilian nuclear power fuel reprocessing, because all actinides, including U, Pu, and minor actinides, should be separated from other nonradioactive components to reduce the volume of high-level nuclear waste. In the past two decades, a group of diamide extractants containing ether linkages between two amide groups (i.e., alkyl-substituted 3-oxa-glutaramide called TROGA) have been of great interest in the area of actinide partitioning. These ligands form actinide complexes that can be effectively extracted from nitric acid solutions into organic solvents, and the stripping of actinides from the amide-containing organic solvents can be easily achieved by diluted acid solutions.[1−12] A few new processes based on alkyl-substituted 3-oxa-glutaramide (TROGA) extractants have been

Received: February 26, 2014
Published: September 4, 2014

   dx.doi.org/10.1021/ic5004484 | *Inorg. Chem.* 2014, 53, 9477−9485

under development for the separation of actinides and some fission products, because of their potential to make the separation processes more efficient and environmentally sustainable.[13−17] The amide ligands consist of only C, H, O, and N, so that they are completely incinerable. As a result, compared to the large amounts of liquid and/or solid radioactive waste generated in the PUREX process, the amount of second-hand radioactive waste generated in the amide-based processes could be significantly reduced. The radiolytic and hydrolytic products of the amides are less detrimental to the separation processes than those organophosphorus acids from the degradation of TBP. Besides, the fission materials for making nuclear weapons, plutonium and neptunium, may be extracted and stripped together with uranium, which prevents fission material from proliferating.

Distribution ratios of actinides in some solvent extraction systems containing TROGA ligands under different conditions have been reported in previous studies. The capability of the tridentate TROGA ligands for the extraction of actinide ions from nitric acids generally decreases in the following order: An(III)/Ln(III) ≫ An(IV) ~ An(VI) > An(V) (which is quite different from those of other neutral extractants, such as CMPO, TRPO, TBP, and DMDBTDMA).[18−21] The latter neutral extractants usually present extraction capability that decreases in the following order: An(IV) ~ An(VI) > An(III)/Ln(III) ≫ An(V) [which can reasonably be explained by the effective charges of +3.2 and +2.2 for UO_2^{2+} and NpO_2^{+}, respectively, along with charges of +4 for An(IV) and +3 for An(III)/Ln(III)].[22] Moreover, analysis based on solvent extraction experiments shows some controversies in the extraction reactions and extracted complexes of Ln(III) and An(III) with TROGA ligands. The extracted complexes are expected to contain three tridentate TROGA ligands surrounding the central Ln(III)/An(III) and providing nine oxygen donors to the ion, which are confirmed by some experimental observations. However, in other cases, the formulas of the complexes are suggested to include the participation of four TROGA molecules.[23] To gain insight into the nature of the complexes of these diamide ligands with actinide ions and to help design more efficient extractants for separating actinides, systematic studies are necessary to obtain thermodynamic parameters (e.g., enthalpy and entropy of complexation) and structural factors (e.g., denticity and steric hindrance) that could affect the stability of the complexes.[24]

In this work, the thermodynamics and structures of the complexes of Nd(III), representing An(III)/Ln(III), with *N,N,N′,N′*-tetramethyl-3-oxa-glutaramide (L^I), *N,N*-dimethyl-3-oxa-glutaramic acid (HL^{II}), and their dicarboxylate analogue, oxydiacetic acid (H_2L^{III}), were studied. The reasons for selecting these ligands are as follows. (1) L^I is the smallest homologue of tetraalkyl-oxa-glutaramides used as extractants in solvent extraction, and the methyl groups give the ligand substantial solubility in aqueous solutions; therefore, complexation can be studied with multiple thermodynamic techniques (potentiometry, spectrophotometry, and calorimetry) in aqueous solutions. (2) HL^{II} is the smallest homologue of dialkyl-oxa-glutaramic acids that represent major hydrolysis and radiolysis products of tetraalkyl-oxa-glutaramides. It also forms complexes with actinides to affect the separation of actinides. (3) H_2L^{III} is the dicarboxylate analogue of L^I and HL^{II}, and the three ligands share the same tridentate functional backbone structure for coordinating to metal ions.

As shown in Scheme 1, with the amide groups of L^I being replaced by one (in HL^{II}) and two (in H_2L^{III}) carboxylate groups, the structure from L^I to HL^{II} and H_2L^{III} changes systematically. Therefore, the trends in thermodynamic parameters obtained for the Nd(III) complexes with these three ligands could provide information about the energetics and driving force of the complexation (e.g., enthalpy, entropy, or both) and help in the design of effective extractants for actinide separation in spent fuel reprocessing and nuclear waste treatment.

Scheme 1. Structurally Related Ligands *N,N,N′,N′*-Tetramethyl-3-oxa-glutaramide (TMOGA, L^I), *N,N*-Dimethyl-3-oxa-glutaramic acid (DMOGA, HL^{II}), and Oxydiacetic Acid (ODA, H_2L^{III})

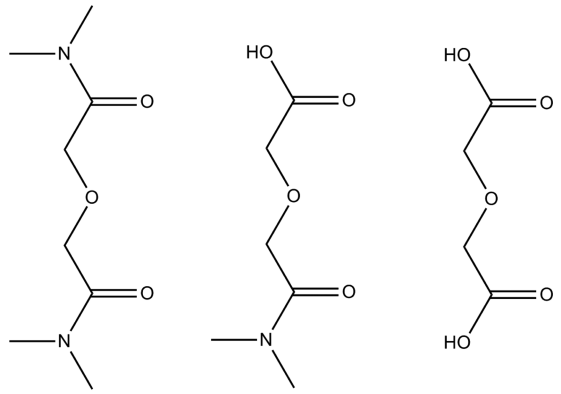

2. EXPERIMENTAL SECTION

2.1. Chemicals. *N,N,N′,N′*-Tetramethyl-3-oxa-gutaramide (L^I) and *N,N*-dimethyl-3-oxa-glutaramic acid (HL^{II}) were previously prepared in this laboratory.[24a,b] Other chemicals were reagent grade or higher.

Milli-Q water was used in preparing all solutions. Nd(III) nitrate/perchlorate stock solutions were prepared by dissolving weighed oxides (Aldrich, 99.9%) with concentrated HNO_3 or $HClO_4$, After the solution had been fumed to near dryness, the residue was redissolved in 1 M HNO_3 or $HClO_4$. The concentrations of Nd(III) and free acid in the stock solution were determined by EDTA titrations and Gran's titration, respectively.[25] Stock solutions of L^I, HL^{II}, and H_2L^{III} were prepared by dissolving appropriate amounts of the ligands in 1 M $NaNO_3$ or $NaClO_4$ solutions. The concentration of L^I was directly calculated from the weight of L^I (MW = 188.23), while the concentrations of HL^{II} and H_2L^{III} (Aldrich, 98%) were determined by potentiometry with a standard carbonate-free NaOH solution. The ionic strength of all solutions used in potentiometry, calorimetry, and spectrophotometry was adjusted to 1.0 M at 25 °C by adding appropriate amounts of sodium perchlorate or nitrate as the background electrolyte.

2.2. Potentiometry. The stability constants of the Nd(III) complexes with HL^{II} (DMOGA) were determined by potentiometric titrations at 25 °C. A detailed description of the titration setup has been provided elsewhere.[26] The titrations were conducted with an automatic titration system consisting of a glass titration cell, a Metrohm pH meter (model 713) equipped with a Ross combination pH electrode (Orion model 8102), a Metrohm dosimat (model 765), and a computer. The temperature of the titration cell was maintained at 25.0 ± 0.1 °C by an external circulating water bath. An inert atmosphere, Ar, was used to prevent the sorption of CO_2 by the solution in the cell during the titration. The original inner solution (3 M KCl) of the electrode was replaced with 1 M NaCl to reduce the

dx.doi.org/10.1021/ic5004484 | Inorg. Chem. 2014, 53, 9477−9485

Table 1. Crystal Data and Structural Refinement for the Nd(III) Complexes

	$Nd(L^{I})_3(ClO_4)_3$ (I)	$Nd(L^{I})_3(NO_3)_3(H_2O)_2$ (II)	$Nd(L^{II})_3(H_2O)_{7.5}$ (III)
chemical formula	$C_{24}H_{48}Cl_3N_6NdO_{21}$	$C_{24}H_{52}N_9NdO_{20}$	$C_{18}H_{45}N_3NdO_{19.50}$
formula weight	1007.27	930.99	759.81
temperature (K)	173(2)	175(2)	150(2)
radiation, wavelength (Å)	synchrotron, 0.77580	synchrotron, 0.77490	synchrotron, 0.77490
crystal system, space group	monoclinic, $C2/c$	monoclinic, $P2_1/c$	triclinic, $P\bar{1}$
unit cell parameters	a = 19.591(3) Å	a = 10.778(3) Å	a = 9.5311(7) Å
	b = 13.366(3) Å	b = 15.662(5) Å	b = 12.2762(9) Å
	c = 15.526(2) Å	c = 23.911(8) Å	c = 13.5139(8) Å
	α = 90°	α = 90°	α = 79.568(2)°
	β = 100.334(6)°	β = 99.735(5)°	β = 80.663(2)°
	γ = 90°	γ = 90°	γ = 87.874(2)°
cell volume (Å^3)	3999.6(11)	3978(2)	1534.42(18)
Z	4	4	2
calculated density (g/cm^3)	1.673	1.554	1.645
absorption coefficient (mm^{-1})	1.99	1.735	2.216
F(000)	2052	1916	780
crystal color and size	pale blue, 0.10 mm × 0.08 mm × 0.08 mm	pale purple, 0.13 mm × 0.12 mm × 0.08 mm	pale purple, 0.08 mm × 0.05 mm × 0.02 mm
no. of reflections for cell refinement	5389 (θ range of 2.30−27.89°)	9697 (θ range of 3.83−33.63°)	4274 (θ range of 2.88−33.49°)
data collection method	Bruker Platinum 200 CCD	Bruker APEX II CCD diffractometer ω rotation with narrow frames	Bruker APEX II CCD diffractometer ω rotation with narrow frames
θ range for data collection (deg)	2.30−27.98	4.16−33.07	2.71−33.69
index ranges	h −24 to 24, k −16 to 16, l −19 to 19	h −15 to 15, k −22 to 22, l −33 to 33	h −13 to 13, k −17 to 17, l −18 to 18
completeness (%)	99.6	98.8	99.1
no. of reflections collected	14996	88264	22758
no. of independent reflections	4078 (R_{int} = 0.0663)	11439 (R_{int} = 0.0552)	8879 (R_{int} = 0.0308)
no. of reflections with $F^2 > 2\sigma$	3740	9526	8059
absorption correction	semiempirical from equivalents	semiempirical from equivalents	semiempirical from equivalents
minimal and maximal transmission	0.83 and 0.86	0.75 and 0.83	0.80 and 0.89
structure solution	direct methods	direct methods	direct methods
refinement method	full-matrix least squares on F^2	full-matrix least squares on F^2	full-matrix least squares on F^2
data/restraints/parameters	4078/0/249	11439/39/492	8879/22/421
final R indices ($F^2 > 2\sigma$)	R1 = 0.0442, wR2 = 0.1195	R1 = 0.0345, wR2 = 0.0923	R1 = 0.0260, wR2 = 0.0652
goodness of fit on F^2	1.059	1.030	1.052
largest and mean shift (su)	0.029 and 0.000	0.002 and 0.000	0.002 and 0.000
largest difference peak and hole (e Å^{-3})	1.081 and −0.817	1.320 and −1.038	1.021 and −1.337

electrode junction potential. Prior to each titration, an acid/base titration with standard HCl and NaOH was performed to calibrate the electrode, so that the EMF readings could be converted into the concentrations of the hydrogen ion in the subsequent titration. Multiple titrations were conducted with solutions of different concentrations ($C_{L^{II}}$, C_H, and C_{Nd}). Forty to 50 data points were collected in each titration. The formation constants of Nd(III)/DMOGA complexes were calculated with Hyperquad 2008.[27]

2.3. Spectrophotometry. Spectrophotometric titrations were conducted on a Cary6000i spectrophotometer from 550 to 620 nm (10 mm cuvette, 1 nm spectral bandwidth, and 0.2 nm data interval) to determine the stability constants of Nd(III) complexes with all three ligands. For a typical titration, 2.0 mL of the Nd(III) solution was put in the cuvette, into which appropriate aliquots of ligand solutions were added, and the solution was mixed thoroughly (for 1−2 min) before the spectrum was collected. Prior kinetic experiments showed that the complexation reaction was fast and the absorbance became stable within 30 s of mixing.

2.4. Calorimetry. An isothermal microcalorimeter (ITC 4200, Calorimetry Sciences Corp.) was used to determine the enthalpies of complexation of Nd(III) complexes with the ligands. Information about the microcalorimeter and its calibration was provided previously.[26] Multiple titrations using different concentrations of the reagents (C_L, C_H, and C_{Nd}) were performed to reduce the uncertainty of the results. The reaction heats measured by microcalorimetry were used, in conjunction with the protonation and complexation constants, to calculate the enthalpies of complexation with HypDeltaH.[28]

2.5. Single-Crystal X-ray Diffractometry. Crystals of 1:3 Nd(III)/L^{I} (nitrate and perchlorate) and Nd(III)/L^{II} complexes were obtained from aqueous solutions by slow evaporation. The X-ray diffraction data were collected at low temperatures using a Bruker Platinum 200 CCD/Bruker APEX II detector with synchrotron radiation at beamline 11.3.1 of the Advanced Light Source at Lawrence Berkeley National Laboratory. Intensity data were collected within 1 h using Bruker Apex 2.[29] Intensity data integrations, cell refinement, and data reduction were performed using the Bruker SAINT software package.[30] Absorption correction was made with SADABS.[31] Dispersion factors (f' and f'') at 16 keV were calculated using CROMER for Windows.[32] The structure was determined with direct methods using SHELXS and refined using SHELXL.[33] Non-hydrogen atoms were refined anisotropically. The hydrogen atoms on carbon atoms were placed geometrically and refined using a riding model. All

dx.doi.org/10.1021/ic5004484 | Inorg. Chem. 2014, 53, 9477−9485

other hydrogen atoms were found in the difference map and allowed to refine freely. The crystal data and structural refinement for the three Nd(III) complexes are listed in Table 1.

3. RESULTS AND DISCUSSION

3.1. Thermodynamic Parameters. *3.1.1. Stability Constants of Nd(III) Complexes.* The stability constants of Nd(III) complexes with all three ligands were determined by spectrophotometry. In addition, the stability constants of Nd(III) complexes with L^{II} were determined by potentiometry, as was determined for Nd(III) complexes with L^{III} in the literature.[34] Acid−base potentiometry cannot be applied to the Nd(III)/L^{I} system because of the absence of dissociable protons in L^{I}.

Figure 1 shows a representative potentiometric titration of the complexation of Nd(III) with L^{II}. The best model to fit the data includes the formation of three successive Nd(III)/L^{II} complexes:

$$Nd^{3+} + n(L^{II})^{-} = Nd(L^{II})_n^{(3-n)+} (n = 1, 2, 3) \quad (1)$$

where $(L^{II})^{-}$ stands for the deprotonated DMOGA. The calculated stability constants for $Nd(L^{II})_n^{(3-n)+}$ are listed in Table 2.

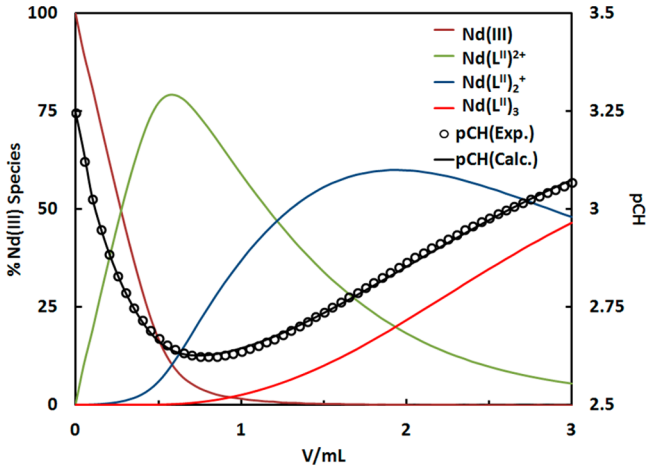

Figure 1. Potentiometric titration of Nd(III) complexation with L^{II} in 1 M $NaClO_4$. Cell solution: V^0 = 40.0 mL, $C_H{}^0$ = 0.60 mM, and $C_{Nd(III)}{}^0$ = 4.58 mM. Titrant solution: C_H = 0.0237 M, and C_L = 0.183 M.

Figure 2 shows representative sets of absorption spectra for the titrations of Nd(III) with L^{I}, L^{II}, and L^{III}. In all titrations, significant changes in the spectra are observed as the concentration of the ligands increases. In particular, the absorption bands of Nd(III) are generally red-shifted, with three new branches of the bands appearing successively, resulting in three isosbestic points in the set of spectra in each titration (the isosbestic points for the three ligand systems are at 575.6, 579.2, and 581.8 nm for L^{I}, 576.0, 579.4, and 581.6 nm for L^{II}, and 576.2, 579.4, and 581.4 nm for L^{III}, respectively). Analysis with Hyperquad indicates that the spectral changes in the titration can be described by successive formation of three Nd(III) complexes. Accordingly, the stability constants were calculated and are listed in Table 2, and the molar absorptivities of the complexes are shown in Figure 2 (bottom row).

As shown in Table 2, the stability constants of the Nd(III)/L^{III} complexes measured by spectrophotometry in this work and by potentiometry in the literature[34] are in fair agreement. Under the experimental condition, only completely deprotonated L^{III} is found in the complexes, in contrast to the $UO_2{}^{2+}$/ODA system in which partially protonated L^{III} was found in the complexes.[35] For the Nd(III)/L^{II} complexes, the stability constants obtained by potentiometry and spectrophotometry agree very well. The titrations of Nd(III)/L^{I}, shown in the left plots of Figure 2, were performed in 1 M $NaNO_3$ instead of 1 M $NaClO_4$, because precipitation occurred in the latter medium because of the low solubility of the perchlorate salt of the Nd/L^{I} complex(es). As a result, the stability constant of the Nd(III)/nitrate complex, $Nd(NO_3)^{2+}$, must be known so that correction can be made to account for the complexation of Nd(III) with nitrate in the spectrophotometric titrations of

Table 2. Complexation of Nd(III) (25 °C)

ligand	method[a]	log β	ΔH (kJ mol^{-1})	ΔS (J K^{-1} mol^{-1})	ref
TMOGA[b]					
$Nd^{3+} + L = NdL^{3+}$	sp, cal	3.53 ± 0.10	−10.9 ± 0.9	26 ± 1	this work
$Nd^{3+} + 2L = NdL_2{}^{3+}$	sp, cal	5.84 ± 0.19	−15.6 ± 1.5	39 ± 2	this work
$Nd^{3+} + 3L = NdL_3{}^{3+}$	sp, cal	6.80 ± 0.19	−19.3 ± 2.2	59 ± 7	this work
DMOGA[c]					
$Nd^{3+} + L^{-} = NdL^{2+}$	pot	5.13 ± 0.18			this work
	sp, cal	4.85 ± 0.17	−6.85 ± 0.37	75 ± 1	this work
$Nd^{3+} + 2L^{-} = NdL_2{}^{+}$	pot	8.49 ± 0.16		120 ± 1	this work
	sp, cal	8.32 ± 0.28	−12.8 ± 0.6		this work
$Nd^{3+} + 3L^{-} = NdL_3(aq)$	pot	10.89 ± 0.22			this work
	sp, cal	10.70 ± 0.27	−14.7 ± 0.8	159 ± 1	this work
ODA[c]					
$Nd^{3+} + L^{2-} = NdL^{+}$	pot, cal	5.45	−3.54	92	34
	sp, cal	5.31 ± 0.14	−3.94 ± 0.24	88 ± 2	this work
$Nd^{3+} + 2L^{2-} = NdL_2{}^{-}$	pot, cal	9.50	−8.79	152	34
	sp, cal	9.28 ± 0.18	−9.90 ± 0.30	145 ± 2	this work
$Nd^{3+} + 3L^{2-} = NdL_3{}^{3-}$	pot, cal	12.16	−12.54	190	34
	sp, cal	12.07 ± 0.21	−14.0 ± 0.6	184 ± 2	this work

[a]Abbreviations: pot, potentiometry; sp, spectrophotometry; cal, calorimetry. [b]I = 1.0 M $NaNO_3$. [c]I = 1.0 M $NaClO_4$.

dx.doi.org/10.1021/ic5004484 | Inorg. Chem. 2014, 53, 9477−9485

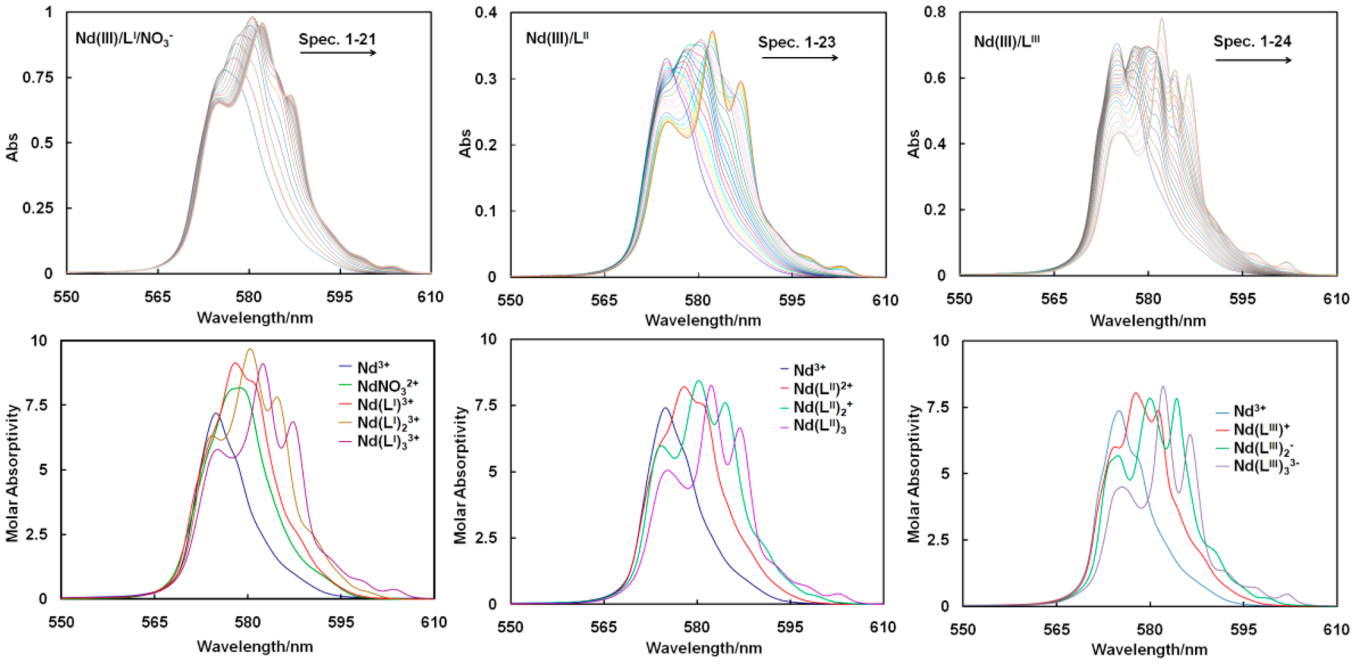

Figure 2. Spectrophotometric titrations of Nd(III) complexation. V^0 = 2.50 mL. Top row: spectra collected during titrations. Bottom row: molar absorptivities obtained from spectral deconvolution. Left: L^I in 1 M $NaNO_3$, $C_{Nd(III)}{}^0$ = 0.110 M; titrant solution, C_L = 1.00 M. Middle: L^{II} in 1 M $NaClO_4$, $C_H{}^0$ = 0.50 mM, $C_{Nd(III)}{}^0$ = 0.0458 M; titrant solution, C_H = 0.014 M, C_L = 0.293 M. Right: L^{III} in 1 M $NaClO_4$, $C_H{}^0$ = 0.0005 mM, $C_{Nd(III)}{}^0$ = 0.0916 M; titrant solution, C_H = 0.014 M, C_L = 0.293 M.

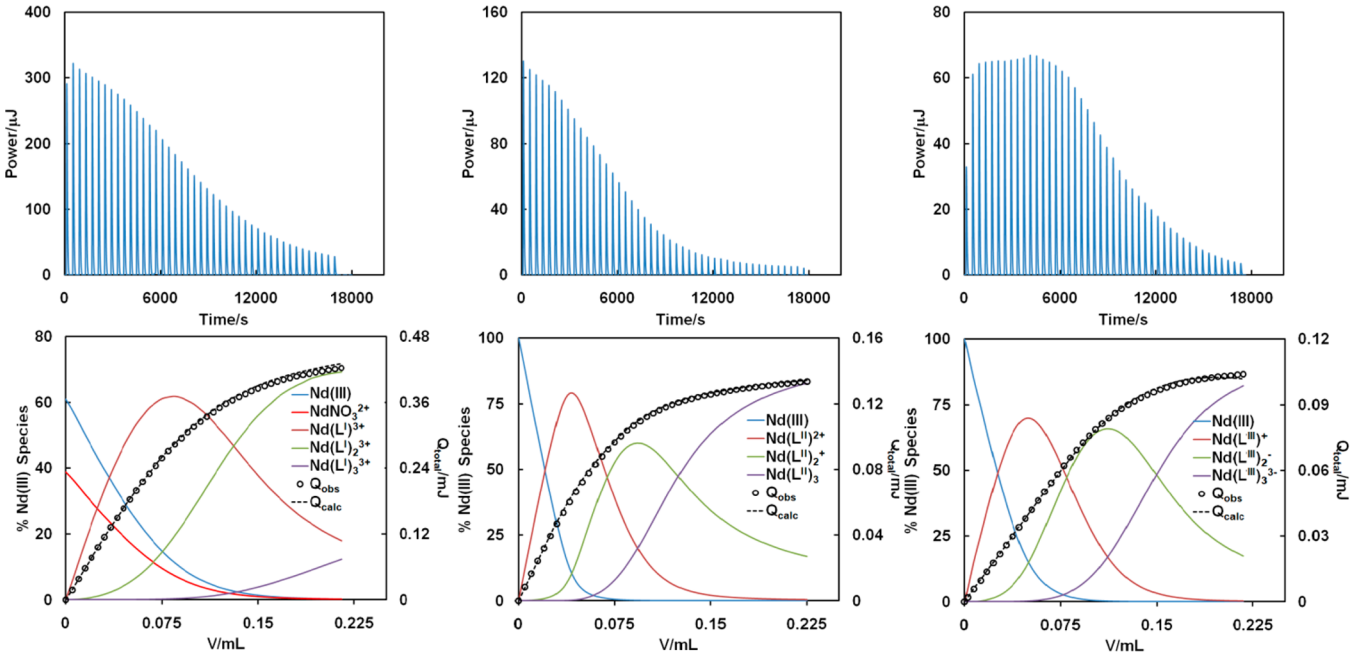

Figure 3. Calorimetric titrations of Nd(III) complexation. V^0 = 0.90 mL, injection volume = 0.005 mL, injection interval = 400 s. Top row: thermograms. Bottom row: corresponding speciation and accumulated heat. Left: I = 1 M $NaNO_3$, $C_{Nd(III)}{}^0$ = 0.0307 M, $C_H{}^0$ = 0.0034 M; titrant, 0.40 M L^I. Middle: I = 1 M $NaClO_4$, $C_{Nd(III)}{}^0$ = 0.0101 M, $C_H{}^0$ = 0.0012 M; titrant, L^{II} in 1 M $NaClO_4$, C_H = 0.228 M, C_L = 0.011 M. Right: I = 1 M $NaClO_4$, $C_{Nd(III)}{}^0$ = 0.0106 M, $C_H{}^0$ = 0.00011 M; titrant, L^{III} in 1 M $NaClO_4$, C_H = 0.04 M, C_L = 0.20 M.

Nd(III)/L^I. A separate set of spectrophotometric titrations with Nd(III)/nitrate were conducted, and the value of log β for $Nd(NO_3)^{2+}$ was determined to be $-(0.19 \pm 0.03)$ [Two values of log β for $Nd(NO_3)^{2+}$ at I = 1.0 M $NaClO_4$, -0.19 ± 0.02[36] and 0.3,[37] were available in the literature. The value from ref 36 has been selected for use because it is consistent with the values at variable ionic strengths in the literature (log β = −0.11 to 0.09 for I = 2−5 M) while the value from ref 37 seems to be too high.] at I = 1 M and t = 25 °C.[36]

3.1.2. Enthalpy of Complexation. Figure 3 shows representative calorimetric titrations of Nd(III) complexation with the three ligands. The overall reaction heat, $Q_{r,i}$, and the speciation of Nd(III) complexes are shown as a function of ligand concentration. From the results of multiple titrations

dx.doi.org/10.1021/ic5004484 | Inorg. Chem. 2014, 53, 9477−9485

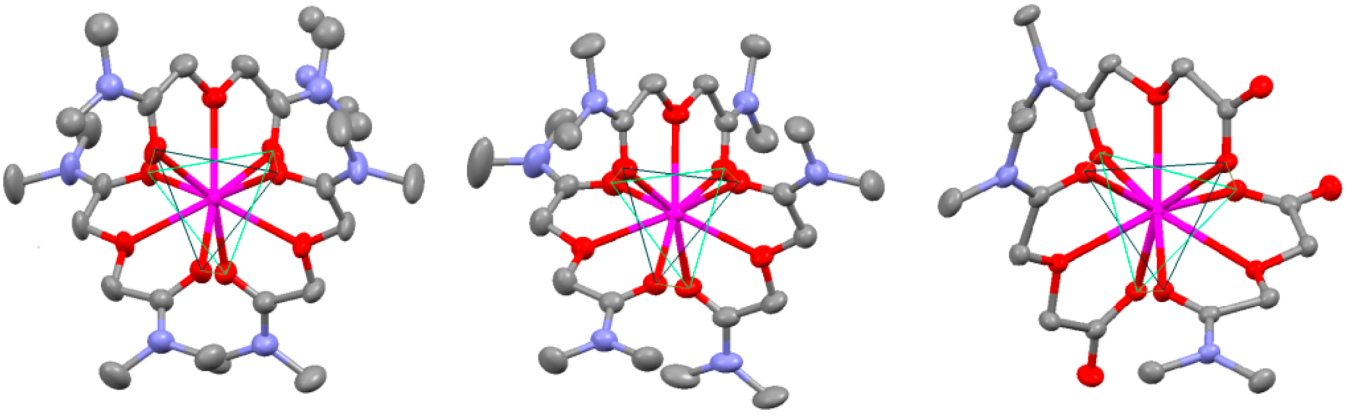

Figure 4. Crystal structures of Nd(III) complexes with 30% probability ellipsoids: (left) $Nd(L^I)_3(ClO_4)_3$, (middle) $Nd(L^I)_3(NO_3)_3(H_2O)_2$, and (right) $Nd(L^{II})_3(H_2O)_{7.5}$. Neodymiums are colored purple, oxygens red, nitrogens blue, and carbons gray. Hydrogen atoms, H_2O molecules, and anions (nitrate/perchlorate ions) have been omitted for the sake of clarity.

with varied Nd(III) and ligand concentrations, the enthalpies of complexation of Nd(III) with the ligands were calculated and are listed in Table 2. A value of ΔH for the $Nd^{3+} + NO_3^- \rightarrow Nd(NO_3)^{2+}$ reaction, determined in a previous study,[36] was used in the calculation for the complexation of Nd(III) with L^I (TMOGA) to correct the contribution of the formation of $Nd(NO_3)^{2+}$ in the titrations.

3.1.3. Thermodynamic Trends. Data in Table 2 show that the complexation of Nd(III) with the ligands becomes weaker upon moving from L^{III} (two $-COO^-$ groups) to L^{II} [one $-COO^-$ group and one $-C(O)N(CH_3)_2$ group] and L^I [two $-C(O)N(CH_3)_2$ groups], which is consistent with the general observation that the negatively charged oxygen of the carboxylic group is a stronger donor to Nd(III) than the oxygen of the neutral amide group. However, opposing trends in the enthalpy and entropy of complexation were observed: from L^{III} to L^{II} and L^I (while the carboxylate groups are replaced with amide groups). The enthalpies of complexation (ΔH) became more exothermic and more favorable for complexation, but the entropy of complexation (ΔS) became less positive and less favorable for complexation. The trend in the enthalpy of complexation from L^{III} to L^{II} and L^I could be explained by the difference in the degree of hydration between the carboxylate group ($-COO^-$) and the amide group [$-C(O)N(CH_3)_2$], the former being more hydrated than the latter. To form complexes with Nd(III), less energy is required to dehydrate the amide group, resulting in more exothermic enthalpy from L^{III} to L^{II}, and further to L^I. For the same argument with respect to the difference in the degree of hydration, the trend in the entropy of complexation could be explained. Upon complexation, fewer water molecules could be released from the hydration sphere of the amide group than from the carboxylate group, resulting in less positive entropy of complexation from L^{III} to L^{II} and L^I. Because the changes in the $T\Delta S$ terms exceeded those in ΔH for these systems, the overall effect was that the stability constants decreased from L^{III} to L^{II} and L^I.

3.1.4. Comparison with U(VI) and Np(V) Complexation and Implications for Separation. Similar trends in the stability constants and enthalpies and entropies of complexation were observed in the complexation of UO_2^{2+} and NpO_2^+ with L^I, L^{II}, and L^{III}.[24b,c] The stability constants of the UO_2^{2+} and NpO_2^+ complexes increased in the following order: $L^I < L^{II} < L^{III}$. The enthalpy of complexation became less exothermic and less favorable for complexation. A similar argument with respect to the difference in the degree of hydration between the ligands discussed for the Nd(III) system could apply to the UO_2^{2+} and NpO_2^+ systems and explain the trends.

We notice that, while the complexation of Nd(III) with the three ligands is all exothermic, the complexation of U(VI)[24b] and Np(V)[24c] with the three ligands is all endothermic. Various factors could probably result in such a difference. For example, the energy for the dehydration of the cations is expected to be different. Besides, the nature of the bonding of these ligands with Ln(III), U(VI), and Np(V) could be different. The question of whether the complexation in these systems can simply be explained by electrostatic interactions remains to be answered.[38]

The thermodynamic data for the complexation of L^I (*N,N,N′,N′*-tetramethyl-3-oxa-glutaramide, TMOGA) with Nd(III), U(VI), and Np(V) could be compared with the distribution data in the solvent extraction of Nd(III), U(VI), and Np(V) with *N,N,N′,N′*-tetraisobutyl-3-oxa-glutaramide (TiBOGA), a homologue of L^I with bulkier alkyl groups that only dissolves in organic solvents. In solvent extraction with TiBOGA, the extracted species were identified as 1:2 U(VI)/TiBOGA, 1:2 Np(V)/TiBOGA, and 1:3 Nd(III)/TiBOGA complexes,[4,9] and the extractability of actinide/lanthanide metal ions (An/Ln) decreased in the following order: An(III)/Ln(III) ≫ An(VI) > An(V).[4] This order agrees with the trend in the stability constants of the metal complexes with L^I in aqueous solutions (log β): $Nd(L^I)_3^{3+}$ (6.80), $UO_2(L^I)_2^{2+}$ (2.94), and $NpO_2(L^I)_2^+$ (2.47). Interestingly, the enthalpies of complexation in aqueous solutions become more endothermic from Nd(III) to U(VI) and Np(V) (ΔH in kilojoules per mole): $Nd(L^I)_3^{3+}$ (−19.3), $UO_2(L^I)_2^{2+}$ (+19.6), and $NpO_2(L^I)_2^+$ (+43.5). This implies that the difference in enthalpy could be the origin of the unusual extraction order of An(III)/Ln(III) ≫ An(VI) > An(V) for the TROGA extractants.

3.2. Structures and Coordination Modes. *3.2.1. Crystal Structures.* Structures of the 1:3 Nd(III) complexes in solid compounds $Nd(L^I)_3(ClO_4)_3$ (**I**), $Nd(L^I)_3(NO_3)_3(H_2O)_2$ (**II**), and $Nd(L^{II})_3(H_2O)_{7.5}$ (**III**) are shown in Figure 4. Selected bond lengths of **I**, **II**, and **III**, as well as those of a Nd(III)/L^{III} complex [**IV**, $Nd(L^{III})_3^{3-}$] from the literature,[39] are listed in Table 3.

3.2.1.1. $Nd(L^I)_3(ClO_4)_3$ (I). The perchlorate salts of the 1:3 Nd(III) complex with L^I crystallized in monoclinic space group

dx.doi.org/10.1021/ic5004484 | Inorg. Chem. 2014, 53, 9477−9485

Table 3. Selected Bond Lengths

	bond length (Å)			
bond	I	II	III	IV[39]
Nd−O (corner)	2.402(3)	2.407(2)	2.4128(15)	2.428
	2.422(3)	2.408(2)	2.4228(15)	
	2.449(3)	2.422(2)	2.4319(16)	
	2.402(3)	2.434(2)	2.4410(15)	
	2.422(3)	2.436(2)	2.4668(15)	
	2.449(3)	2.439(2)	2.4702(15)	
average	2.424(3)	2.424(5)	2.423(4)	2.428
Nd−O (capping)	2.526(4)	2.515(2)	2.5537(15)	2.523
	2.533(3)	2.522(2)	2.5623(14)	
	2.533(3)	2.549(2)	2.6066(14)	
average	2.531(6)	2.529(3)	2.574(3)	2.523

$C2/c$. There are four molecules of the $Nd(L^{I})_3^{3+}$ complex and 12 molecules of the perchlorate counterion in the C-centered unit cell. The trivalent ion Nd(III), one coordinating ether oxygen atom of one L^{I}, and one perchlorate lie on the crystallographic 2-fold axis at [0, y, 0.25].

3.2.1.2. $Nd(L^{I})_3(NO_3)_3(H_2O)_2$ (II). The nitrate salt of the 1:3 Nd(III)/L^{I} complex crystallizes in monoclinic space group $P2_1/c$. There are four molecules of the $Nd(L^{I})_3^{3+}$ complex, 12 nitrate counterions, and eight molecules of water in the unit cell.

3.2.1.3. $Nd(L^{II})_3(H_2O)_{7.5}$ (III). The neutral 1:3 Nd(III)/L^{II} complex crystallizes in triclinic space group $P\bar{1}$. There are two molecules of the mononuclear $Nd(L^{II})_3$ complex and 15 molecules of water in the unit cell.

In the three solid complexes, no matter how different the component is, the nine-coordinated Nd(III) always has a distorted tricapped trigonal prism geometry with three ether oxygen atoms capped on the three faces of the prism, and six oxygen atoms from the ketone group or carboxyl group at the corners. The two triangular faces are slightly rotated relative to each other. The Nd(III) center and the three capping ether oxygen atoms are coplanar. The three ligands almost keep the planar backbone structure through non-hydrogen atoms.

In compound **I**, the two positions associated with the methyl carbon atoms and nitrogen were observed in a difference Fourier map and were included with isotropic thermal parameters. The occupancies for these disordered atoms were set at one-half. In addition, all perchlorate anions were found to be disordered. The perchlorate that is located in a general position showed disorder in two of the oxygen atoms. These were included in calculated positions at half-occupancy for each atom within the disorder. The second perchlorate that lies on the 2-fold axis was found to be disordered about the axis. The chlorine is located just off-axis and, subsequently, so are the oxygen atoms. Refinement of the oxygen occupancies revealed that one has an occupancy of 67%, with a smaller, 33% disorder site off the 2-fold axis; the three remaining oxygen atoms are disordered over four positions in addition to being disordered across the 2-fold axis. As the complex has no hydrogen bond donors, acceptors, or π interactions, the structure is essentially comprised of isolated complexes surrounded by perchlorate counterions that sit in the voids between the complexes. A packing structure of compound **I** viewed down the b-axis is shown in Figure 5. The packing structures of this compound viewed down the a-axis and c-axis are shown in the Supporting Information (Figures S1 and S2, respectively).

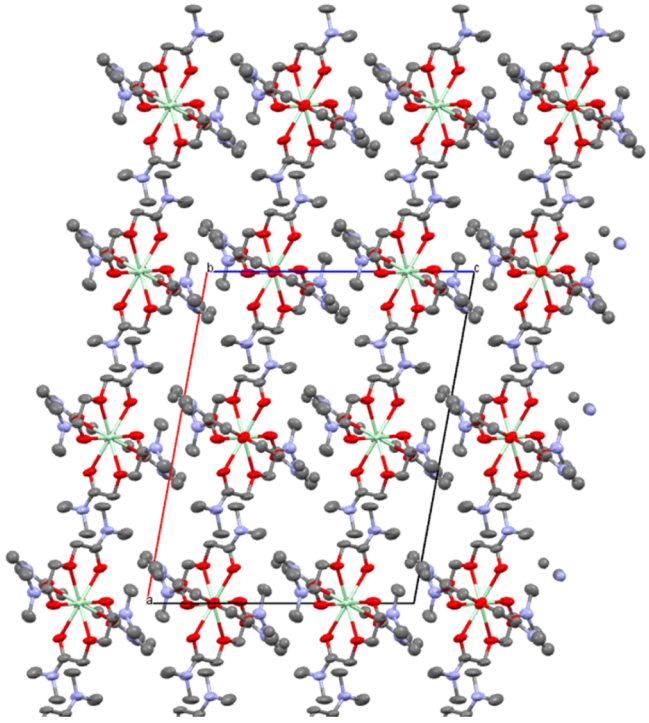

Figure 5. Packing structure of compound **I** viewed down the b-axis, showing the isolated nature of the complex. Hydrogen atoms and perchlorates have been omitted for the sake of clarity. Oxygens are colored red, carbons gray, neodymiums light green, and nitrogens blue.

For compound **II**, the crystal structure is composed of layers along the $b-c$ plane, containing the $Nd(L^{I})_3^{3+}$ complexes and one water and one nitrate, alternating with layers containing the other water and the other two nitrate counterions. The non-hydrogen atoms of each ligand in addition to the Nd(III) center are approximately coplanar. One nitrate is disordered in the layer that is composed of one water and two nitrate ions. As the complex has no hydrogen bond donors, acceptors, or π interactions, the structure is essentially comprised of isolated complexes surrounded by hydrogen-bonded networks of nitrate counterions and waters, such that the complex sits in the voids in this network. A packing structure of compound **II** viewed down the a-axis is shown in Figure 6. The packing structures of this compound viewed down the b-axis and c-axis are shown in the Supporting Information (Figures S3 and S4, respectively).

For compound **III**, the crystal structure is composed of layers along the $a-c$ plane, containing the neutral $Nd(L^{II})_3$ complexes and water molecules, alternating with layers containing other water molecules. It is noteworthy that the three oxygen atoms from the carboxylate groups per $Nd(L^{II})_3$ unit point outside of the mononuclear unit and form hydrogen bonds with the water molecules. The structure consists of corrugated layers of the complex in the $a-c$ plane and is held together by weak $\pi-\pi$ interactions. Some of the waters are hydrogen bonded into pockets in these layers. These layers are bridged by a network of waters hydrogen bonded to the layers through the unbound carboxylate oxygen and themselves. A packing structure of compound **III** viewed down the c-axis is shown in Figure 7. The packing structures of this compound viewed down the a-axis and b-axis are shown in the Supporting Information (Figures S5 and S6, respectively).

3.2.2. Comparison of the Structures. As shown in Figure 4, in all the 1:3 Nd(III)/L complexes, Nd(III) atoms possess very

dx.doi.org/10.1021/ic5004484 | Inorg. Chem. 2014, 53, 9477−9485

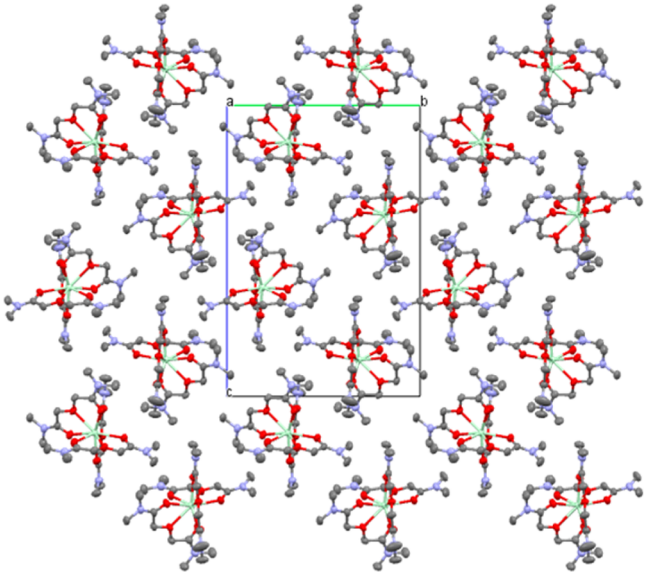

Figure 6. Packing structure of compound **II** viewed down the *a*-axis, showing the isolated nature of the complex. Hydrogen atoms, nitrates, and waters have been omitted for the sake of clarity. Oxygens are colored red, carbons gray, neodymiums light green, and nitrogens blue.

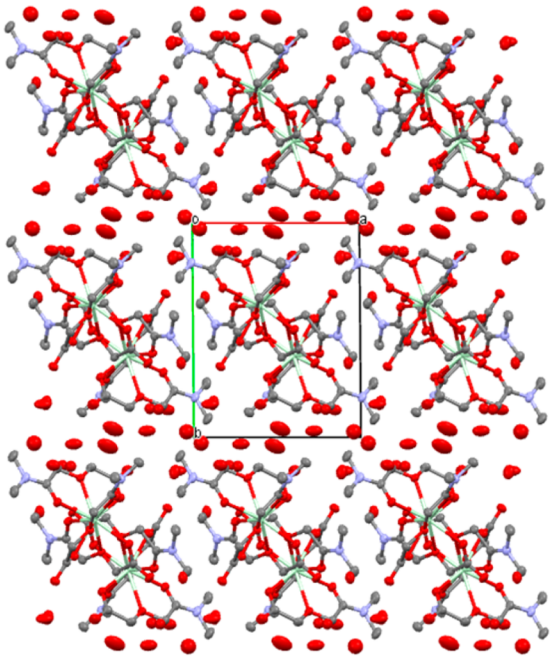

Figure 7. Packing structure of compound **III** viewed down the *c*-axis, showing the layers of the $Nd(L^{II})_3$ complex and waters. Hydrogen atoms have been omitted for the sake of clarity. Oxygens are colored red, carbons gray, neodymiums light green, and nitrogens blue.

similar TCTP geometry, which may originate from the identical rigid backbone structure of the three ligands. There is no clear correlation between the trend of the stability constants measured in aqueous solutions and the O−Nd bond length in the four related solid complexes, including **I**, **II**, and **III** in this work and **IV** $[Nd(L^{III})_3^{3-}]$ from the literature.[39] The average O−Nd bond lengths for the corner oxygen in the four complexes are almost identical. For the capping oxygen in **I**, **II**, and **IV**, the average O−Nd bond lengths are almost the same, regardless of the charge in the ligand or the complex. The average O−Nd bond for the capping oxygen in **III** $[Nd(L^{II})_3(H_2O)_{7.5}]$ is the longest, though L^{II} has a charge of −1, between the charge on L^{I} of 0 and the charge on L^{III} of −2. These observations suggest that the charge on the donor oxygen atoms may not be a deciding factor determining the length and strength of the coordination bond in this system. Instead, the geometry or symmetry of the ligands plays an important role in the formation of the coordination bond for the ligands under study.

For the two Nd(III)/L^{I} complexes [**I** and **II** (Figure 4)], perchlorate and nitrate, the two TCTPs are almost identical, and the type of outer counterions has very little effect on the structure of the complexes, implying that, for the solvent extraction using TROGA as the extractant, the nitrate extracted into the organic phase may not directly bond to the metal ions and behave just as the counterion to balance the charge.

It is interesting to compare structures **I**−**IV** with a crystal structure of $[LaL_3][La(NO_3)_6]$ (where L stands for a TROGA ligand, *N*,*N*,*N*′,*N*′-tetraisobutyl-3-oxa-glutaramide) reported in the literature,[40] taking into consideration that La has an ionic radius larger than that of Nd and the isobutyl group is larger and/or bulkier than the methyl group. The $[LaL_3]^{3+}$ cation moiety consists of a nine-coordinated La center surrounded by three tridentate TROGA ligands in a D_3 symmetry. In a manner similar to that of the structures of **I**−**IV**, the central ether oxygen atom of the ligands takes the capping positions of a twisted TTP geometry. The cationic species $[LaL_3]^{3+}$ was found to associate with a homoleptic counteranion, $[La(NO_3)_6]^{3-}$, for charge balance.

3.2.3. Implication for the Structures of the Complexes in Solution. In addition to the almost identical core nine-coordinated Nd(III) structure in **I**−**IV**, the variation of the hypersensitive absorption band of Nd(III) around 580 nm also presents an almost identical pattern in the spectrophotometric titrations with the three ligands, implying that the corresponding complexes of Nd(III) with the three ligands in aqueous solutions also possess very similar geometry that is, probably, identical to that in the solid crystals.

4. CONCLUSION

The complexation of Nd(III) with three tridentate ligands, TMOGA, DMOGA, and ODA, was studied in both solution and the solid state. For all three ligands, 1:1, 1:2, and 1:3 Nd(III)/ligand complexes were identified in 1 M $NaNO_3$ or 1 M $NaClO_4$. The stability constants for corresponding complexes of the three ligands with Nd(III) decrease in the following order: ODA > DMOGA > TMOGA. The complexation for all complexes was driven by both enthalpy and entropy. The almost identical deconvoluted spectra from the titrations in solution imply that the coordination geometries of the corresponding Nd(III) complexes with the three ligands in aqueous solutions are similar. The coordination geometries of Nd(III) in three solid compounds prepared in this work and an Nd(III)/ODA complex in the literature are also very similar. In these complexes, the nine-coordinated Nd(III) sits at the center of a distorted tricapped trigonal prism with three ether oxygen atoms capped on the three faces of the prism, and six oxygen atoms from the ketone group or carboxyl group at the corners. All three ligands are tridentate. The Nd−O bond distances do not show a clear dependence on the types of coordinating groups, either the amide or carboxylate groups.

dx.doi.org/10.1021/ic5004484 | *Inorg. Chem.* 2014, 53, 9477−9485

■ ASSOCIATED CONTENT

Supporting Information

Crystallographic information files (CIF) and packing structures of compounds **I**–**III** viewed down different axes. This material is available free of charge via the Internet at http://pubs.acs.org.

■ AUTHOR INFORMATION

Corresponding Authors

*E-mail: sjteat@lbl.gov.
*E-mail: lrao@lbl.gov.

Notes

The authors declare no competing financial interest.

■ ACKNOWLEDGMENTS

This work was supported by the Director of the Office of Science, Office of Basic Energy Science of the U.S. Department of Energy (DOE), under Contract DE-AC02-05CH11231 at Lawrence Berkeley National Laboratory. Single-crystal X-ray diffraction data were collected and analyzed at the Advanced Light Source (ALS). ALS is supported by the Director of the Office of Science, Office of Basic Energy Sciences of the DOE, under Contract DE-AC02-05CH11231.

■ REFERENCES

(1) Sasaki, Y.; Choppin, G. *Radiochim. Acta* **1998**, *80*, 85–88.
(2) Suzuki, H.; Sasaki, Y.; Sugo, Y.; Apichaibukol, A.; Kimura, T. *Radiochim. Acta* **2004**, *92*, 463–466.
(3) Ansari, S. A.; Pathak, P. N.; Husain, M.; Prasad, A. K.; Parmar, V. S.; Manchanda, V. K. *Radiochim. Acta* **2006**, *94*, 307–312.
(4) Tian, G.; Zhang, P.; Wang, J.; Rao, L. *Solvent Extr. Ion Exch.* **2005**, *23* (5), 631–643.
(5) Nave, S.; Modolo, G.; Madic, C.; Testard, F. *Solvent Extr. Ion Exch.* **2004**, *22* (4), 527–551.
(6) Narita, H.; Yaita, T.-i.; Tachimori, S. *Solvent Extr. Ion Exch.* **2004**, *22* (2), 135–145.
(7) Shimada, A.; Yaita, T.; Narita, H.; Tachimori, S.; Okuno, K. *Solvent Extr. Ion Exch.* **2004**, *22* (2), 147–161.
(8) Sasaki, Y.; Sugo, Y.; Tachimori, S. *Solvent Extr. Ion Exch.* **2001**, *19* (1), 91–103.
(9) Tian, G.; Wang, J.; Song, C. *He Huaxue Yu Fangshe Huaxue* **2001**, *23* (3), 135–140.
(10) Sugo, Y.; Sasaki, Y.; Tachimori, S. *Radiochim. Acta* **2002**, *90*, 161–165.
(11) Tian, G.; Zhang, P.; Shen, Y.; Wang, J.; Rao, L. *Solvent Extr. Ion Exch.* **2005**, *23* (4), 519–528.
(12) Tian, G.; Zhang, P.; Shen, Y.; Wang, J.; Rao, L. *Sep. Sci. Technol.* **2012**, *47* (14–15), 2160–2165.
(13) Ansari, S. A.; Pathak, P.; Mohapatra, P. K.; Manchanda, V. K. *Chem. Rev.* **2012**, *112* (3), 1751–1772.
(14) Magnusson, D.; Christiansen, B.; Glatz, J.; Malmbeck, R.; Modolo, G.; Purroy, D.; Sorel, C. *Solvent Extr. Ion Exch.* **2009**, *27*, 26.
(15) Geist, A.; Modolo, G. TODGA process development: An improved solvent formulation. *In Proceedings of International Conference GLOBAL 2009*, Paris, September 6–11, 2009; Paper 9193, pp 1022–1026.
(16) Gujar, R. B.; Ansari, S. A.; Prabhu, D. R.; Pathak, P. N.; Sengupta, A.; Thulasidas, S. K.; Mohapatra, P. K.; Manchanda, V. K. *Solvent Extr. Ion Exch.* **2012**, *30* (2), 156–170.
(17) Tachimori, S.; Sasaki, Y.; Morita, Y.; Suzuki, S. Recent progress of partitioning process in JAERI: Development of amide-based ARTIST process. In *Proceedings of the 7th Information Exchange Meeting on Actinide and Fission Product Partitioning and Transmutation*, Jeju, Korea, October 14–16, 2002.
(18) Horwitz, E. P.; Kalina, D. G.; Kaplan, L.; Mason, G. W.; Diamond, H. *Sep. Sci. Techol.* **1982**, *17*, 1261–1279.
(19) Zhu, Y.; Jiao, R. *Nucl. Technol. (Chinese)* **1994**, *108*, 361–370.
(20) Murali, M. S.; Mathur, J. N. *Solvent Extr. Ion Exch.* **2001**, *19*, 61–67.
(21) Cuillerdier, C.; Musikas, C.; Nigond, L. *Sep. Sci. Technol.* **1993**, *28*, 155–175.
(22) Choppin, G. R.; Rao, L. *Radiochim. Acta* **1984**, *37*, 143–146.
(23) Jensen, M. P.; Yaita, T.; Chiarizia, R. *Langmuir* **2007**, *23* (9), 4765–4774.
(24) (a) Tian, G.; Xu, J.; Rao, L. *Angew. Chem., Int. Ed.* **2005**, *44* (38), 6200–6203. (b) Tian, G.; Rao, L.; Teat, S.; Liu, G. *Chem.—Eur. J.* **2009**, *15* (16), 4172–4181. (c) Rao, L.; Tian, G.; Teat, S. *Dalton Trans.* **2010**, *39* (13), 3326–3330.
(25) Gran, G. *Analyst* **1952**, *77*, 661.
(26) Rao, L.; Srinivasan, T. G.; Garnov, A. Yu.; Zanonato, P.; Di Bernardo, P.; Bismondo, A. *Geochim. Cosmochim. Acta* **2004**, *68*, 4821.
(27) Gans, P.; Sabatini, A.; Vacca, A. *Talanta* **1996**, *43*, 1739.
(28) Gans, P.; Sabatini, A.; Vacca, A. *J. Solution Chem.* **2008**, *4*, 467.
(29) *Apex2*; Bruker Analytical X-ray Systems, Inc.: Madison, WI, 2003.
(30) *SAINT: SAX Area-Detector Integration Program*, version 7.60a; Bruker Analytical X-ray Systems, Inc.: Madison, WI, 2010.
(31) Blessing, R. H. *Acta Crystallogr.* **1995**, *A51*, 33.
(32) Kissel, W. L.; Pratt, R. H. *Acta Crystallogr.* **1990**, *A46*, 170.
(33) Sheldrick, G. M. *Acta Crystallogr.* **2008**, *A64*, 112.
(34) Grenthe, I. *Acta Chem. Scand.* **1963**, *17*, 2487–2498.
(35) Rao, L.; Garnov, A.; Jiang, J.; Di Bernardo, P.; Zanonato, P.; Bismondo, A. *Inorg. Chem.* **2003**, *42* (11), 3685–3692.
(36) Rao, L.; Tian, G. *Inorg. Chem.* **2009**, *48*, 964–970.
(37) Martell, A. E.; Smith, R. M. *Critical Stability Constants*; Plenum: New York, 1977; Vol. 3 (First Supplement, 1982; Second Supplement, 1989).
(38) Jensen, M.; Nash, K. *Radiochim. Acta* **2001**, *89*, 557–564.
(39) Albertsson, J. *Acta Chem. Scand.* **1970**, *24*, 3527–3541.
(40) Kannan, S.; Moody, M. A.; Barnes, C. L.; Duval, P. B. *Inorg. Chem.* **2008**, *47*, 4691.